Anion Conformation and Physical Properties in BETS Salts with the Nitroprusside Anion and its Related Ruthenium Halide (X = Cl, Br) Mononitrosyl Complexes: θ-$(BETS)_4[Fe(CN)_5NO]$, $(BETS)_2[RuBr_5NO]$, and $(BETS)_2[RuCl_5NO]$

Maria-Elena Sanchez,[a] Marie-Liesse Doublet,[b] Christophe Faulmann,[a] Isabelle Malfant,*[a] Patrick Cassoux,[a] Lyudmila A. Kushch,[c] and Eduard B. Yagubskii[c]

Keywords: Sulfur heterocycles / Ruthenium / Halides / Conducting materials / Electronic structure

θ-$(BETS)_4[Fe(CN)_5NO]$ (**1**), $(BETS)_2[RuBr_5NO]$ (**2**), and $(BETS)_2[RuCl_5NO]$ (**3**) [BETS = bis(ethylenedithio)tetraselenafulvalene] have been prepared by electrocrystallisation of BETS using $[Fe(CN)_5NO]^{2-}$ or $[RuX_5NO]^{2-}$, X = Cl or Br, as supporting electrolytes and 1,1,2-TCE/ethanol (10 vol%) for **1**, nitrobenzene/1,2-DCE (40 vol%)/ethanol (10 vol%) for **2**, and benzonitrile/ethanol (10%) solutions for **3** as solvents. Compound **1** exhibits a metallic behaviour down to 40 K, **2** behaves as a semiconductor and **3** as an insulator. The crystal structures of **1**, **2**, and **3** were determined by X-ray diffraction methods. BETS molecules in **1** crystallised in a θ-type mode. By contrast, the crystal structures of **2** and **3** show a packing of BETS molecules consisting of slipped, stacked $(BETS)_2$ dimers. The dimerisation is much stronger in **3** than in **2**. The physical behaviours of the three phases were investigated by means of molecular and band structure calculations and are shown to be directly related to the $[MX_5NO]$ (M = Fe, X = CN; M = Ru, X = Cl, Br) structural conformations.

Introduction

A recent new development in the research on molecular conductors concerns the possibility of creating solids in which conductivity (or superconductivity) coexists with other physical phenomena. This novel class of multifunctional materials should provide a unique opportunity to study the competition and mutual influence of, and better still a possible interplay between two properties in the same crystal lattice. Until recently, attention along this line has been primarily directed towards magnetic conductors.[1]

A parallel approach involving conducting radical cation salts with photochromic anions has been explored even more recently. The interest in the synthesis and characterisation of new molecular conductors containing photochromic anions is to analyse the influence of the electronic excitation of the anions over the conducting (superconducting) electrons. For example, one can imagine the design of a photochromic molecular conductor (or even a superconductor) in which the conducting properties can be tuned by light. In this context, the use of the photochromic nitroprusside $[Fe(CN)_5NO]^{2-}$ anion and related mononitrosyl transition-metal complexes as counter-anions in radical cation salts of BEDT-TTF [BEDT-TTF = bis(ethylenedithio)tetrathiafulvalene] and its analogues has been contemplated.[2,3] These anions are highly interesting because they possess extremely long-living metastable excited states at low temperatures that can be generated by laser irradiation.[4] Two-dimensional salts in which BEDT-TTF or its oxygen-substituted analogue BEDO-TTF [BEDO-TTF = bis(ethylenedioxy)tetrathiafulvalene] is associated with the $[Fe(CN)_5NO]^{2-}$ anion have been already reported, as well as salts with the TTF molecule.[2]

The BETS molecule [BETS = bis(ethylenedithio)tetraselenafulvalene] is a modification of BEDT-TTF obtained by substituting selenium for sulfur in the central tetrathiafulvalene fragment (Figure 1).[5] A strikingly large number of metal-like and superconducting BETS-based salts have been recently reported.[6] Thus, BETS-based conducting salts incorporating photochromic anions also seem to be promising candidate systems for the preparation of photochromic conductors and superconductors.[3]

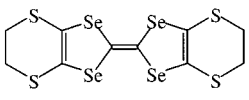

Figure 1. Atomic scheme for BETS

We report here on the preparation, the crystal and electronic structures, and the solid state properties of three phases namely, θ-$(BETS)_4[Fe(CN)_5NO]$ (**1**), $(BETS)_2[RuBr_5NO]$ (**2**), and $(BETS)_2[RuCl_5NO]$ (**3**), obtained when using the appropriate $[Fe(CN)_5NO]^{2-}$, $[RuBr_5NO]^{2-}$, $[RuCl_5NO]^{2-}$ anions.

[a] Laboratoire de Chimie de Coordination, CNRS, 205 route de Narbonne, 31077 Toulouse cedex, France
[b] Laboratoire de Structure et Dynamique des Systèmes Moléculaires et Solides USTL II, Place E. Bataillon, 34095 Montpellier cedex 5, France
[c] Institute of Problems of Chemical Physics in Chernogolovka, Russian Academy of Sciences, Chernogolovka, 142432 Russia

  1434–1948/01/1111–2797 $ 17.50+.50/0

Results and Discussion

Synthesis and Electrical Properties

Three different phases are obtained when the BETS molecule is associated with the $[Fe(CN)_5NO]^{2-}$ anion and its substituted mononitrosylruthenium halide $[RuX_5NO]^{2-}$ (X = Cl or Br) complexes. All these phases have been obtained electrochemically and characterised by X-ray structure determination and energy-dispersive X-ray spectrometry (EDS).[3b]

The different molecular arrangements of **1**, **2**, and **3** lead to different physical behaviours. The single-crystal room-temperature conductivity of **1** is 0.01 $S\cdot cm^{-1}$. As depicted in Figure 2, the temperature-dependent resistance shows a weakly metallic behaviour down to ca. 40 K ($\sigma_{40\,K}$ = 0.07 $S\cdot cm^{-1}$). Below this temperature, the compound undergoes a metal-to-semiconductor phase transition. By contrast, **2** is a semiconductor (0.2 $S\cdot cm^{-1}$) with a very small activation energy (E_a = 0.03 eV), whereas **3** behaves as an insulator, its resistivity at room temperature being larger than $4\cdot10^3$ $\Omega\cdot cm$.

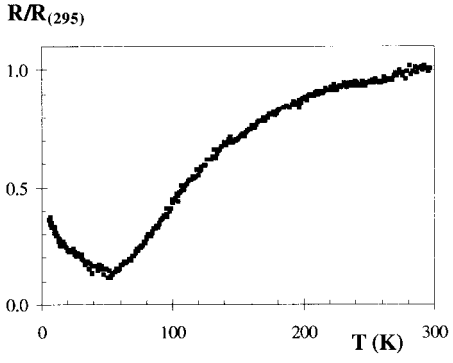

Figure 2. Temperature dependence of the resistance in **1**

X-ray Structure of 1, 2, and 3

θ-(BETS)$_4$[Fe(CN)$_5$NO] (1)

The asymmetric unit contains half a BETS molecule lying on a centre of inversion and 1/8 $[Fe(CN)_5NO]$ entity lying on a twofold rotation axis. The complete determination of the anion has not been possible because of a strong disorder: Two Fe atoms [Fe(1) and Fe(2)] are located at about 2 Å from each other along the twofold axis. This leads to a very low electronic density for the C, N, and O atoms whose positions could not be determined. Only one crown of electron density is evidenced from the Fourier map, which leads to the representation of the anion shown in Figure 3, a. A similar, not resolved disorder of the nitroprusside anion has also been observed in (BEDO-TTF)$_4$[Fe(CN)$_5$NO].[2c]

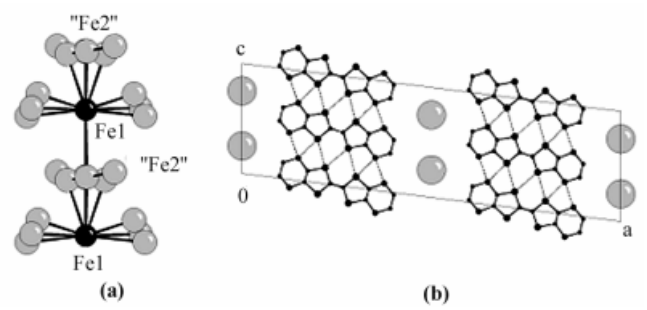

Figure 3. Cameron view of the anion in **1** along the *b* axis (a); projection in the *ac* plane of the cationic layer of **1** (b); the grey circles represent the electronic densities of the nitroprusside anion, H atoms are omitted for clarity

The crystal structure of **1** consists of sheets of adjacent columns in the *bc* plane alternating with layer of anions along the *a* direction (Figure 3, b). Two equivalent $(BETS)_2$ layers occur in the unit cell. Within each layer, the BETS molecules stack in a θ-type mode (Figure 4).[7] They form chains of parallel BETS molecules, running along the *b* direction and connected to adjacent chains through short chalcogen···chalcogen contacts (Table 1). The dihedral

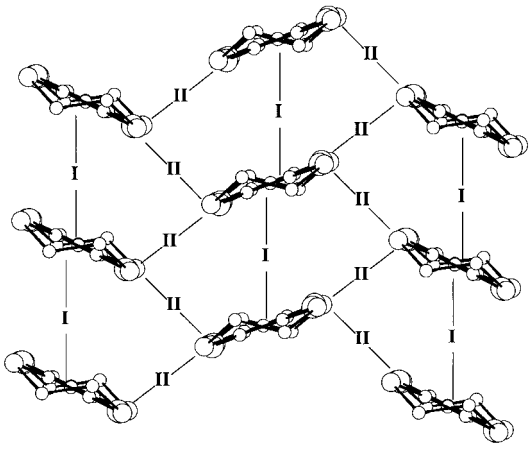

Figure 4. Projection of the cationic layer of **1** along the BETS central C=C bond, H atoms are omitted for clarity

Table 1. Se···Se distances smaller than 4.2 Å and absolute values of the $\beta_{HOMO\text{-}HOMO}$ interaction energies [eV] for the different BETS−BETS interactions in **1**, **2**, and **3** [see Figures 4, 5 (a), and 7 (a) for labelling of **1**, **2**, and **3**, respectively]

	Se ··· Se [Å]	$\beta_{HOMO\text{-}HOMO}$ [eV]
3	3.479(1) (× 2)[a]	β_{intra} = 1.274
	3.596(1) (× 2)[a]	
	4.145(1) (× 2)[b]	β_{inter} = 0.316
2	3.513(5)[c]	β_{intra} = 0.623
	3.890(5)[d], 3.994(5)[d]	β_{inter} = 0.323
1	4.072(1) (× 2)[e], 4.178(1) (× 2)[e]	β_I = 0.158
	3.734(2) (× 4)[f], 3.792(2) (× 4)[g],	β_{II} = 0.094
	3.813(2) (× 4)[h]	

[a] Symmetry operations: $1-x, -y, 1-z$. [b] $2-x, -y, 1-z$. [c] x, y, z. [d] $1+x, y, z$. [e] $x, -1+y, z$. [f] $x, -y, -0.5+z$. [g] $x, 1-y, -0.5+z$. [h] $0.5-x, -0.5+y, 2.5-z$.

angle between two BETS molecules belonging to adjacent chains is 133.82°.

$(BETS)_2[RuBr_5NO]$ (2)

The asymmetric unit contains two BETS molecules and one $[RuBr_5NO]$ entity. As shown in Figure 5, the packing consists of chains of dimerised BETS molecules (the distance between the averaged planes of two BETS molecules belonging to one dimer is 0.512 Å shorter than the distance between two dimeric entities) stacking along the *a* direction with Se···Se and Se···S contacts shorter than the van der Waals distances (Figure 5, a). The crystal structure of **2** can be described as a pseudo-hexagonal columnar architecture made of short intra- and intermolecular chalcogen···chalcogen contacts. The anionic complexes are located in the centre of each hexagon and repeat infinitely along the *a* direction (Figure 5, b).

In this phase, the anionic complex is pseudo-octahedral with averaged Ru−Br distances of 2.466(7) Å and

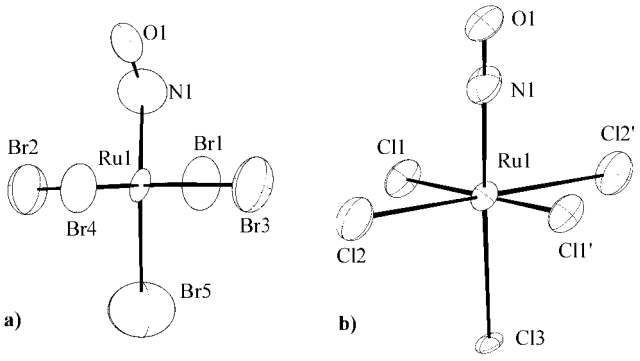

Figure 6. Cameron view of the anionic part in **2** (a) and **3** (b)

Br−Ru−Br angles close to 90° for the planar (Ru1Br1Br2Br3Br4) entity. The Ru−Br5 apical bond is almost perpendicular to the $Ru(Br)_4$ plane (89.20°). On the other hand, the Ru−N−O angle is 160.0(5)° (Figure 6, a). As already studied, this non-linearity can be connected with

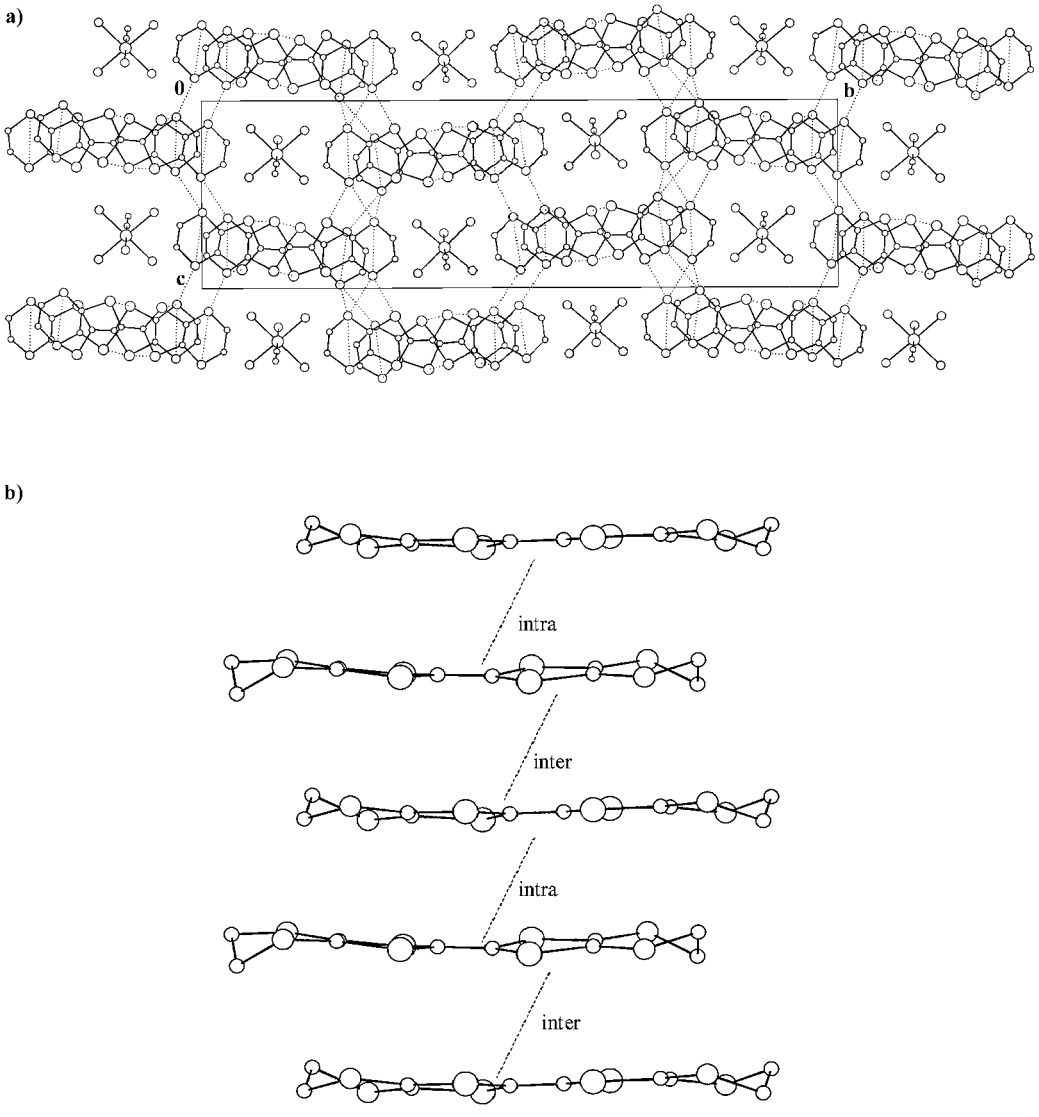

Figure 5. Projection in the *bc* plane of **2** (a); chain of BETS molecules along the *a* axis (b); H atoms are omitted for clarity

the formal charge on the nitrosyl ligand.[8] This will be discussed later in the discussion of the electronic structure.

$(BETS)_2[RuCl_5NO]$ (3)

The asymmetric unit contains one BETS molecule and half a $[RuCl_5NO]$ entity lying on a centre of inversion. Due to this special position, the nitrosyl ligand and the Cl(3) atom have an occupancy of 0.5 and are equally distributed on both sides of the Ru atom. The BETS molecule adopts a chair conformation, as shown in Figure 7, a. The crystal structure of **3** consists of chains of strongly slipped dimerised BETS molecules (built from two eclipsed BETS molecules connected through short Se···Se contacts, Table 1) stacking along the *a* direction and alternating with the anion along the *b* direction. Several chalcogen···chalcogen contacts shorter than the van der Waals distances occur between dimers belonging to the adjacent stacks (Figure 7, b). Thus, the structure can be regarded as sheets in the $(01\bar{1})$ plane of interconnected chains of isolated BETS dimers separated by $RuCl_5NO$ anions along the $[01\bar{1}]$ direction.

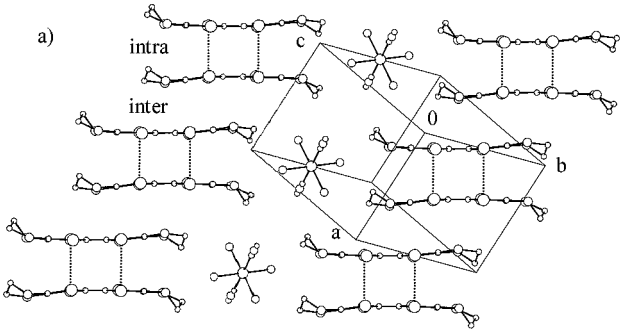

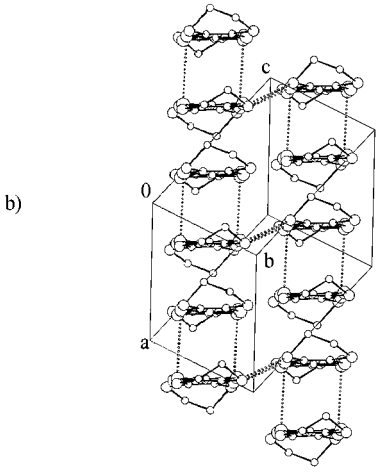

Figure 7. Projection in the $(01\bar{1})$ plane of **3** (a); projection of the cationic layer of **3** along the BETS central C=C bond (b); H atoms are omitted for clarity

As in **2**, the anionic complex presents a pseudo-octahedral configuration with averaged equatorial Ru−Cl distances of 2.381(2) Å and angles between Ru, Cl atoms, and NO ligand close to 90°. Contrary to **2**, Ru−N−O is almost linear [178.0(3)°] (Figure 6, b). This linearity will be discussed in the next part and compared to the bent conformation of $RuBr_5NO$ in **2**.

Electronic Structure of 1, 2, and 3

$(BETS)_2[RuX_5NO]$ (X = Br, Cl) (2, 3)

The intermolecular interaction energies calculated between the highest occupied molecular orbital (HOMO) of two adjacent BETS molecules are reported in Table 1. They confirm that **2** and **3** are characterised by strongly dimerised BETS chains running along the *a* direction of the crystal lattice, all inter-chain interactions being smaller by at least one order of magnitude. It is in agreement with the non-metallic properties of the BETS layers in **2** and **3**.

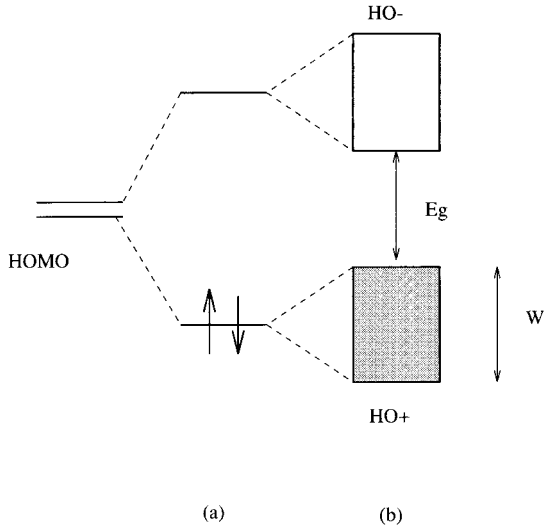

Figure 8. Qualitative electronic band structure of a strongly dimerised one-dimensional molecular solid; (a) and (b) correspond to the dimer and solid electronic structures, respectively; W and E_g stand for the bandwidths and the energy band gap, respectively

As depicted in Figure 8, the band structure of a dimerised chain consists of a fully occupied low-lying band (HO^+) and an empty high-lying band (HO^-). These two bands originate from the molecular orbitals $\Psi \cong^{+}_{HOMO}$ and $\Psi \cong^{-}_{HOMO}$ of the dimer, i.e. from the symmetric and the antisymmetric linear combinations between the HOMOs of the two interacting monomers.

The HO^+ and HO^- bandwidths (W) as well as the energy gap (E_g) between these two bands are governed by the inter-dimer and the intra-dimer interaction energies, namely β_{inter} and β_{intra}. In the case of **2** and **3**, the strong dimerisation observed in the BETS layers results in rather high band gaps ($E_g \approx 0.6$ eV for **2** and $E_g \approx 1.2$ eV for **3**) and small bandwidths, supporting their non-metallic behaviours.

However, whereas a large band gap is in agreement with the insulating behaviour of **3**, it is not consistent with the very small experimental activation energy $E_a = 0.03$ eV determined for **2**. To understand this discrepancy between experimental and theoretical results, it may be useful to pay

closer attention to the electronic structure of the anions, from which the following explanation may be proposed.

As previously mentioned, the main difference between the $[RuBr_5NO]^{2-}$ and the $[RuCl_5NO]^{2-}$ anions concerns the Ru−N−O angle α (see Figure 5). Whereas NO is linearly bonded to the ruthenium metal centre for X = Cl [α = 178.0(3)°], it is bent with an angle α = 160.0(5)° for X = Br. The subtle π-electron transfers occurring between the ruthenium atom and a bent or a linear NO ligand are well known and have been shown to depend on the nature of the ancillary ligands.[8] In particular, it has been shown that the Ru−N−O angle can be correlated to the π-donor character of the remaining ligands through a three-centre four-electron interaction, and that the nitrosyl formal charge can thus be treated as negative NO^- for a bent NO (α = 120°) and positive NO^+ for a linear one.[8] As a consequence, different Ru−N−O angles may result in different formal oxidation states for the transition metal atom. It is therefore tempting to associate the bending angle observed in the $(BETS)_2[RuBr_5NO]$ salt with a more pronounced π-donor character of Br^- compared to that of Cl^-. However, the nature of X (X = Cl or Br) does not seem to be the only factor that governs the nitrosyl conformation. Indeed, the Ru−N−O bending angles in $K_2[RuBr_5NO]$ and $K_2[RuCl_5NO]$ are nearly equivalent [α = 174.4(1)° for X = Br and α = 176.7(5)° for X = Cl].[9] Thus, the different bending angles in **2** and **3** raise the possibility that the BETS layers may interact with the anions, at the very least in **2**.

Considering further the Ru−N−O bending angles reported in the $(BETS)_2[RuBr_5NO]$ (X = Cl, Br) salts, a positive NO^+ may be conceived for X = Cl (α = 178°) and an intermediate charge between NO^+ and NO^- for X = Br (α = 160°). This would result in different oxidation states for the transition metal in the two compounds. Whereas for X = Cl, the $[Ru^{II}Cl_5^{5-}NO^+]^{2-}$ formal electron count is fully consistent with the insulating properties of a strongly dimerised $(BETS)_2^{2+}$ cationic layer, it may be envisioned that for X = Br some of the electron density missing around the transition metal (Ru^{+n}; $n > 2$) is retained by the cationic layers.

This hypothesis leads to the presence of some few electrons in the weakly dispersive HO^- band of the BETS layers, and is consistent with the very small activation energy experimentally measured for **2**. Hence, the different physical properties of $(BETS)_2[RuCl_5NO]$ and $(BETS)_2[RuBr_5NO]$ are proposed to originate from different BETS−RuX_5NO interactions, leading to different BETS→RuX_5NO electron transfers and therefore to different Ru oxidation states. EPR measurements are in progress to obtain more insight along this line. It should be noticed, however, that preliminary results have already shown a large and asymmetric signal centred at $g = 2.037$ for **2**, and no EPR signal for **3**. Such a large signal for **2** is unlikely to be the signature of isolated $BETS^+$ radicals, but is in turn consistent with our hypothesis of a Ru^{n+} ($n > 2$) oxidation state in the $(BETS)_2[RuBr_5NO]$ salt.

$(BETS)_4[Fe(CN)_5NO]$ (1)

Unlike Cl^- and Br^-, CN^- is a strong π-acceptor ligand. Consequently, the metal-like molecular orbitals of a $[Fe(CN)_5NO]$ pseudo-octahedron are expected to be less occupied, for an equivalent NO bending angle, than in the analogous $[RuX_5NO]$ (X = Cl, Br) complexes. The nitrosyl ligand most likely adopts a linear conformation to compensate (at least partially) for the lack of electron density around the transition metal centre. This seems to be corroborated by the strong disorder reported for the $[Fe(CN)_5NO]$ anions, since X-ray diffraction techniques often encounter difficulties in distinguishing close atoms such as C, N and O. Hence, to stabilise an Fe^{II} formal oxidation state,[10] the anions of **1** should require a larger electron density from the BETS layers than in the other Ru-based phases, in agreement with the 4:1 stoichiometry observed for that salt.

Since no accurate information on the anionic layers is available, the electron transfer cannot be accurately determined here. The electronic band structure and the Fermi surfaces associated with different oxidation states of the $(BETS)_2^{\rho+}$ ($\rho = 1, {}^3/_2$) cationic slabs are presented in Figure 9. Although $BETS^{+1/2}$ corresponds to the usual oxidation state found in BETS-based metal-like salts, it appeared interesting to check whether a larger oxidation state ($BETS^{+3/4}$) could alter the Fermi surface of the salt.

The electronic structures of Figure 9 are very similar to those previously reported for the homologous θ-type BETS phase associated with $[Cu_2Cl_6]^{2-}$ anions.[11] According to the topology of the intermolecular interactions (see Table 1), the Fermi surface associated with ρ = 1 exhibits a two-dimensional character (2D). This is consistent with the observed metallic behaviour of **1** at room temperature but cannot explain the first-order phase transition observed

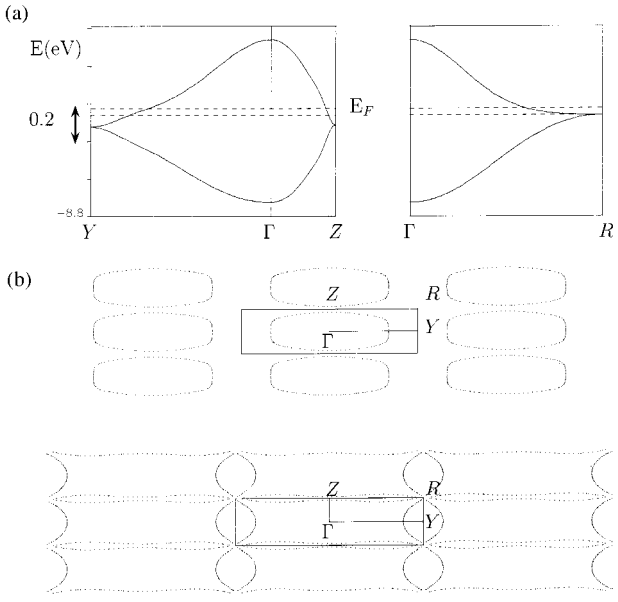

Figure 9. Electronic band structure of **1** (a), the dotted lines refer to the Fermi levels for ρ = 1 and ρ = ${}^3/_2$; Fermi surfaces of one $(BETS)_2^{\rho+}$ layer of **1** (b) for ρ = 1 (top) and ρ = ${}^3/_2$ (bottom); Γ, Y, Z and R correspond to the wave vectors (0,0), (b*/2,0), (0,c*/2) and (b*/2,c*/2), respectively

around 40 K, since such a 2D character of the Fermi surface would suggest a stable metallic state for this compound down to low temperatures. Should a larger electron transfer ($\rho = {}^{3}/_{2}$) be considered, then the Fermi level would approach the two degenerated HOMOs (see Figure 9, a).

As already suggested in a previous work,[11b] slight changes in the donor slab could occur at low temperature due to a modification of the donor−acceptor interactions. Such structural changes could be responsible for the change in the resistivity behaviour around 40 K. Let us note, however, that among all presently known BETS and BEDT-TTF cation radical based organic conductors, it is not rare that a first-order phase transition cannot be rationalised in terms of electronic instabilities of the Fermi surface. In a very recent work,[12] Canadell et al. suggested that the first-order phase transition observed in the κ-$(BETS)_2C(CN)_3$ salt mainly involves the anionic slabs and that the electronic structure of the donor slabs is only slightly altered by the transition. To obtain more insights into the mechanism of the transition observed for **1**, low-temperature X-ray investigations as well as magnetoresistance measurements could be of interest. The former may help in determining which of the cationic or/and anionic slabs is affected by the transition, and the latter may allow us to properly determine the electron transfer occurring from the donor slabs to the $[Fe(CN)_5NO]$ species, for this charge transfer is directly related to the area of the 2D Fermi surface.

Conclusions

The use of the nitroprusside $[Fe(CN)_5NO]^{2-}$ anion and its related mononitrosylruthenium halide complexes $[RuX_5NO]^{2-}$ (X = Cl, Br) in the preparation of BETS-based salts led to a number of different phases with different stoichiometries, **1**, **2**, and **3**. These various phases exhibit different interesting structures and properties. Compound **1** exhibits a metallic behaviour down to 40 K where it undergoes a first-order metal-to-semiconductor phase transition. Compound **2** is a small activated semiconductor ($E_a = 0.03$ eV) and **3** is an insulator. Molecular and band structure calculations have been carried out to rationalise the physical properties of the three salts. The results suggest a direct role of the anionic slabs on the electronic properties of the BETS layers. The different physical behaviours of **2** and **3**, corresponding to the same 2:1 stoichiometry, have been correlated to the conformation of the $[RuX_5NO]$ (X = Cl, Br) species. Depending on the Ru−N−O bending angle, different oxidation states are expected for the ruthenium atom and therefore different electron transfers from the BETS layers to the $[RuX_5NO]$ species. When NO is linearly bonded to the transition metal centre, the stabilisation of an $[Ru^{II}Cl_5NO^+]^{2-}$ anion dictates an integral oxidation state for the BETS molecules, in agreement with the insulating behaviour of **3**. When NO bends, a formal intermediate charge between NO^+ and NO^- may be considered, yielding an Ru^{n+} ($n > 2$) oxidation state. The lack of electron density around the transition metal centre is thus proposed to be retained by the BETS layers, in agreement with the small activation energy of **2**. Due to the 2D character of the $(BETS)_2^{1+}$ Fermi surface calculated for **1**, it is likely that the phase transition occurring in this compound mainly involves the anionic slabs. Nevertheless, low-temperature crystallographic data are required to check whether the donor slabs are, or are not affected by the phase transition.

In conclusion, this work has revealed possible relationships between the anion conformation and the physical properties of **1**, **2**, and **3**. We have shown that the presence of the radical cation salts affects the geometry of the nitroprusside anion and its related mononitrosylruthenium halide complexes $[RuX_5NO]^{2-}$ (X = Cl, Br). Further studies are currently in progress to investigate the photochromic properties of these systems, including DSC measurements to detect the existence of long-lived metastable states in the nitrosyl complexes, and Mössbauer experiments as well as conductivity measurements under irradiation.

Experimental Section

Syntheses: $(PPh_4)_2[Fe(CN)_5NO]$ was obtained by reaction of $Na_2[Fe(CN)_5NO]$ (Aldrich) with $(Ph_4P)Cl$ in water. $K_2[RuX_5NO]$ (X = Cl or Br) were synthesised according to the method of Mercer.[13] $(NH_4)_2[RuBr_5NO]$ was obtained by reaction of $K_2[RuBr_5NO]$ and NH_4Cl. − Crystals of **1** were obtained by electrocrystallisation from BETS solutions in 1,1,2-trichloroethane/ethanol (10 vol%) at 50 °C. $(Ph_4P)_2[Fe(CN)_5NO]$ was used as supporting electrolyte. The donor ($4\cdot10^{-4}$ M) and the electrolyte ($3\cdot10^{-3}$ M) were introduced into the different compartments of an H-shaped electrochemical cell. Oxidation of the donor was performed electrochemically (constant current density, $i = 0.5$ μA·cm^{-2}). Within 5 d, black crystals of **1** (thick blocks) grew on the anode, together with some few other diamond- and hexagonal-plate-shaped phases. − Crystals of **2** and **3** were obtained by using the same general procedure adding 18-crown-6 ($4\cdot10^{-3}$ M for **2** and $7\cdot10^{-3}$ M for **3**, respectively) with concentrations of the donor of $3\cdot10^{-4}$ M for **2** and $6\cdot10^{-4}$ M for **3**, respectively. $(NH_4)_2[RuBr_5NO]$ ($2\cdot10^{-3}$ M) and $K_2[RuCl_5NO]$ ($7\cdot10^{-3}$ M) were used as supporting electrolytes in nitrobenzene/1,2-dichloroethane (40 vol%)/ethanol (10%) for **2** and in benzonitrile/ethanol (10%) solutions for **3**. Crystals of **2** grew on the anode within 20 d (50 °C, $i = 0.5$ μA·cm^{-2}) while crystals of **3** (38 °C, $i = 1.5$ μA·cm^{-2}) grew within one month. − Conductivity measurements were performed using the standard four-probe method between room temperature and 4 K. Electrical contacts were achieved by mounting crystals on a Motorola printed circuit and gluing four gold wires on the sample with gold paint.

X-ray Crystallographic Studies: The experimental details and crystal data are listed in Table 2. The structures were solved using direct methods (SHELXS 97)[14] (**1** at 160 K, **2** at 160 K, and **3** at 193 K) and refined using full-matrix least squares on F^2. The calculations were carried out with the CRYSTALS[15] and WINGX[16] package programs running on a PC. The drawings of the molecular structures were obtained with the help of CAMERON.[17] The atomic scattering factors were taken from the International Tables for X-ray Crystallography.[18] Crystallographic data (excluding structure factors) for the structures reported in this paper have been deposited with the Cambridge Crystallographic Data Centre as supplementary publication no. CCDC-158312 (**1**), -158313 (**2**), -158314 (**3**). Copies of the data can be obtained free of charge on applica-

Table 2. Crystal data for **1**, **2**, and **3**

	θ-(BETS)$_4$[Fe(CN)$_5$NO] (**1**)	(BETS)$_2$[RuBr$_5$NO] (**2**)	(BETS)$_2$[RuCl$_5$NO] (**3**)
Empirical formula	$C_{45}H_{32}FeN_6OS_{16}Se_{16}$	$C_{20}H_{16}Br_5NORuS_8Se_8$	$C_{20}H_{16}Cl_5NORuS_8Se_8$
M	2504.92	1675.16	1452.90
Crystal system, space group	monoclinic, $C2/c$	monoclinic, $P2_1/c$	triclinic, $P\bar{1}$
a [Å]	40.259(8)	7.480(1)	8.858(2)
b [Å]	4.1768(7)	41.065(4)	10.367(2)
c [Å]	11.599(2)	12.514(1)	11.351(2)
α [°]	90	90	110.52(1)
β [°]	97.23(2)	105.00(1)	97.46(1)
γ [°]	90	90	105.46(2)
V [Å^3]	1934.9(6)	3713.0	911.7(3)
Z	1	4	1
$d_{calcd.}$ [g·cm^{-3}]	2.15	3.03	2.65
F(000)	1178	3124	680
μ(Mo-K_α) [cm^{-1}]	81.87	141.2	92.64
Data collection			
Temperature [K]	160	160	193
Diffractometer	Stoe IPDS	Stoe IPDS	Bruker Smart CCD
Scan mode	Φ	Φ	Φ and ω
Scan range Φ [°]	$0 < \Phi < 250$	$0 < \Phi < 250$	Φ = 0, 90, 180 with $-28 < \omega < 152$
No. of collected reflns.	5841	12560	14536
No. of unique reflns.	1251	2683	14536
No. of reflns. used	1013 [$I > 2\sigma(I)$]	2683 [$I > 2\sigma(I)$]	10347 [$I > 2\sigma(I)$]
R	0.082	0.0845	0.0588
wR_2	0.223	0.2674	0.1524
No. of parameters	87	397	223

tion to CCDC, 12 Union Road, Cambridge CB2 1EZ, UK [Fax: (internat.) + 44-1223/336-033; E-mail: deposit@ccdc.cam.ac.uk].

Band-Structure Calculations: The electronic band structures of the cationic layers were investigated using full tight-binding calculations based upon the effective one-electron Hamiltonian of the extended Hückel model.[19] The off-diagonal matrix elements of the Hamiltonian β_{ij} were calculated according to the modified Wolfsberg−Helmholz formula.[20] All valence electrons were explicitly treated in the calculations and the basis set, consisting in double-ζ Slater-type orbitals for C, S, Se and single-ζ Slater-type orbitals for H were taken from previous work.[11b]

Acknowledgments

The authors thank Dr. H. Gornitzka for recording data of **3**, D. Berail from Motorola Company for supplying printed circuits for conductivity measurements. M. E. S. V. thanks the CONACYT and the Instituto Tecnológico y de Estudios Superiores de Monterrey, Campus Ciudad de México for a postdoctoral grant. Support from CNRS and the Foundation for Basic Research, through an International Program for Scientific Cooperation (PICS), is gratefully acknowledged.

[1] [1a] M. Kurmoo, A. W. Graham, P. Day, S. J. Coles, M. B. Hursthouse, J. L. Caulfield, J. Singleton, F. L. Pratt, W. Hayes, L. Ducasse, P. Guionneau, *J. Am. Chem. Soc.* **1995**, *117*, 12209−12217. − [1b] P. Day, *C. R. Acad. Sci. Paris, série IIc* **1999**, *2*, 675−684, and references therein. − [1c] L. Brossard, R. Clerac, C. Coulon, M. Tokumoto, T. Ziman, D. K. Petrov, V. N. Laukhin, M. J. Naughton, A. Audouard, F. Goze, A. Kobayashi, H. Kobayashi, P. Cassoux, *Eur. Phys. J. B1* **1998**, 439−452, and references therein. − [1d] H. Kobayashi, A. Kobayashi, P. Cassoux, *Chem. Soc. Rev.* **2000**, *29*, 325−333. − [1e] E. Coronado, J. R. Galan-Mascaros, C. J. Gomez-Garcia, V. Laukhin, *Nature* **2000**, 447−449.

[2] [2a] L. Kushch, L. Buravov, V. Tkacheva, E. Yagubskii, L. Zorina, S. Khasanov, R. Shibaeva, *Synth. Met.* **1999**, *102*, 1646−1649. − [2b] M. Gener, E. Canadell, S. S. Khasanov, L. V. Zorina, R. P. Shibaeva, L. A. Kushch, E. B. Yagubskii, *Solid State Commun.* **1999**, *111*, 329−333. − [2c] L. V. Zorina, S. S. Khasanov, R. P. Shibaeva, M. Gener, R. Rousseau, E. Canadell, L. A. Kushch, E. B. Yagubskii, O. O. Drozdova, K. Yakushi, *J. Mater. Chem.* **2000**, *10*, 2017−2023. − [2d] M. Clemente-Leon, E. Coronado, J. R. Galan-Mascaros, C. Gimenez-Saiz, C. J. Gomes-Garcia, J. M. Fabre, *Synth. Met.* **1999**, *103*, 2279−2282 − [2e] M. Clemente-Leon, E. Coronado, J. R. Galan-Mascaros, C. J. Gomez-Garcia, E. Canadell, *Inorg. Chem.* **2000**, *39*, 5394−5397.

[3] [3a] P. Cassoux, C. Faulmann, B. Garreau de Bonneval, I. Malfant, S. Aonuma, M. E. Sanchez, *Synth. Met.*, in the press. − [3b] T. Courcet, Doctoral thesis. Université Paul Sabatier, Toulouse, France, **1999**.

[4] [4a] T. Woike, W. Krasser, P. Bechthold, S. Haussühl, *Phys. Rev. Lett.* **1984**, *53*, 1767−1770. − [4b] H. Zöllner, T. Woike, W. Krasser, S. Haussühl, *Z. Kristallogr.* **1989**, *188*, 139−153. − [4c] T. Woike, S. Haussühl, *Solid State Commun.* **1993**, *86*, 333−337. − [4d] M. R. Pressprich, M. A. White, V. Vekhter, P. Coppens, *J. Am. Chem. Soc.* **1994**, *116*, 5233−5238. − [4e] M. D. Carducci, M. R. Pressprich, P. Coppens, *J. Am. Chem. Soc.* **1997**, *119*, 2669−2678.

[5] [5a] R. Kato, H. Kobayashi, A. Kobayashi, *Synth. Met.* **1991**, *41−43*, 2093−2096. − [5b] T. Courcet, I. Malfant, P. Cassoux, *New J. Chem.* **1998**, 585−589.

[6] H. Kobayashi, H. Tomita, T. Naito, A. Kobayashi, F. Sakai, T. Watanabe, P. Cassoux, *J. Am. Chem. Soc.* **1996**, *118*, 368−377.

[7] The symbol θ designates a characteristic and specific type of crystal packing often encountered in BEDT-TTF radical salts; see: J. M. Williams, J. R. Ferraro, R. J. Thorn, K. D. Carlson, U. Geiser, H. H. Wang, A. M. Kini, M. H. Whangbo, *Organic*

Superconductors (including fullerenes), Prentice-Hall, Inc., Englewood Cliffs, New Jersey 07632, **1992**.

[8] M. Ogasawara, D. Huang, W. E. Streib, J. C. Huffman, N. Gallego-Planas, F. Maseras, O. Eisenstein, K. G. Caulton, *J. Am. Chem. Soc.* **1997**, *119*, 8642−8651.

[9] [9a] J. T. Veal, D. J. Hodgson, *Inorg. Chem.* **1972**, *11*, 1420−1424. − [9b] Y. N. Mikhailov, A. S. Kanishcheva, A. A. Svetlov, *Zh. Neorg. Khim.* **1989**, *34*, 2803−2806.

[10] Indeed, the Fe^{II} oxidation state is indicated by preliminary Mössbauer experiments: A. Bousseksou, personal communication.

[11] [11a] A. Kobayashi, A. Sato, E. Arai, H. Kobayashi, C. Faulmann, N. Kushch, P. Cassoux, *Solid State Commun.* **1997**, *6*, 371−374. − [11b] I. Malfant, T. Courcet, C. Faulmann, P. Cassoux, H. Gornitzka, F. Granier, M.-L. Doublet, P. Guionneau, J. A. K. Howard, N. D. Kushch, A. Kobayashi, *C. R. Acad. Sci.* **2001**, *4*, 149−160.

[12] B. Z. Narymbetov, E. Canadell, T. Togonidze, S. S. Khasanov, L. V. Zorina, R. P. Shibaeva, H. Kobayashi, *J. Mater. Chem.* **2001**, *11*, 332−336.

[13] E. E. Mercer, W. M. Campbell, R. M. Wallace, *Inorg. Chem.* **1963**, *3*, 1018−1024.

[14] G. M. Sheldrick, *SHELX97 − Programs for Crystal Structure Analysis* (Release 97-2), Institut für Anorganische Chemie der Universität, Tammanstrasse 4, Göttingen, Germany, **1998**.

[15] D. J. Watkin, C. K. Prout, J. R. Carruthers, P. W. Betteridge, *CRYSTALS*, issue 10, Chemical Crystallography Laboratory, University of Oxford, Oxford, England, **1996**.

[16] *WINGX*, Main Reference; L. J. Farrugia, *J. Appl. Crystallogr.* **1999**, *32*, 837−838.

[17] D. J. Watkin, C. K. Prout, L. J. Pearce, *CAMERON*, Chemical Crystallography Laboratory, University of Oxford, Oxford, England, **1996**.

[18] D. T. Cromer, J. T. Waber, *International Tables for X-ray Crystallography*, Kynoch Press, Birmingham, **1974**, vol. 4.

[19] R. Hoffmann, *Chem. Phys.* **1963**, *39*, 1397−1412.

[20] [20a] J. H. Ammeter, H. B. Bürgi, J. Thibeault, R. Hoffmann, *J. Am. Chem. Soc.* **1978**, *100*, 3686−3692. − [20b] M. H. Whangbo, R. Hoffmann, *J. Am. Chem. Soc.* **1978**, *100*, 6093−6098.

Received March 1, 2001
[I01075]